ARTICLES

Tunable Aggregation and Luminescence of Bis(diarylethene)sexithiophenes

Maaike T. W. Milder[†] and Jennifer L. Herek[†,‡]

FOM Institute for Atomic and Molecular Physics, Kruislaan 407, 1098 SJ Amsterdam, The Netherlands, and Optical Sciences Group, Department of Science and Technology, MESA+ Institute for Nanotechnology, University of Twente, 7500 AE, Enschede, The Netherlands

Jetsuda Areephong, Ben L. Feringa, and Wesley R. Browne*

Centre for Systems Chemistry, Stratingh Institute for Chemistry and Zernike Institute for Advanced Materials, Faculty of Mathematics and Natural Sciences, University of Groningen, Nijenborgh 4, 9747 AG, Groningen, The Netherlands

Received: December 24, 2008; Revised Manuscript Received: May 11, 2009

Diarylethenes with two different side groups (phenyl and chloro) were appended to both α-ends of a sexithiophene unit. The temperature dependent aggregation properties for both compounds were characterized by steady state and transient absorption spectroscopy. The peripheral side groups show an unexpectedly significant influence on the electronic properties of the sexithiophene core. Furthermore, the relative influence of the phenyl and chloro substituents on the aggregation behavior observed is remarkable. The phenyl compound exhibits formation of H-aggregates over a narrow temperature range, between 240 and 200 K, typical of strong intermolecular interactions. In contrast, the chloro compound shows gradual aggregation over a wide temperature range, forming H-aggregates albeit with weaker intermolecular interactions. The results demonstrate that minor changes in the structure lead to tunability of the aggregation and corresponding luminescence properties of sexithiophenes in solution and hold particular relevance to supramolecular and polymer systems based on sexithiophene units.

Introduction

Since the discovery of conducting polymers by Heeger and MacDiarmid in the late 1970s,[1] π-conjugated systems have seen increasing application in areas as diverse as supramolecular chemistry and organic electronics in FETs,[2] OLEDs,[3] molecular wires,[4] photovoltaic cells[5] and electrochromic materials.[6,7] Oligothiophenes[8] in particular show remarkable optical and electronic properties. Their widespread use is due to their stability toward molecular oxygen and water.[9] From a supramolecular perspective, oligothiophenes are especially attractive as components in molecular devices where they can act as bridging units, i.e., molecular wires, between functional units, as well as active components in their own right.[10] The distinct advantage that oligothiophenes provide over their polymeric analogues is their precisely defined structure. Furthermore, in contrast to conventional semiconducting materials, subtle structural changes can yield dramatic effects in conductivity and luminescence properties.[11–14] Whereas in polythiophene the material properties are affected by kinks and bends in their structures, oligothiophenes can form rigid, well-ordered structures more easily. The type of order determines the luminescence and electronic properties of oligothiophenes, providing the tunability required for application in optoelectronic devices.[15–18]

A wide range of substituted oligothiophenes have been reported,[19] in solution, as well as in thin films and single crystals, with sexithiophene-based systems receiving the most attention.[20–22] The properties of oligothiophenes can be tuned via synthetic modification and processing.[23,24] The impact of strong intermolecular interactions between oligothiophenes on solubility typically requires that long alkyl side chains are employed to improve solubility and/or control aggregation. However, while such an approach improves solubility and processability, the steric interactions introduced by the alkyl side chains at the β positions impact on the photophysical and electronic properties in comparison to nonsubstituted oligothiophenes.[25] An alternative approach is to modify oligothiophenes by end-capping the α,α-positions with functional groups, for instance, to control aggregation.[26] This approach limits the steric hindrance and therefore the effects of functionalization on electronic and spectroscopic properties. A further extension is the introduction of added functionality such as photochromism to change the conjugation path length of oligothiophenes.[27–30]

Recently, we have reported[31] the synthesis and photochemical and electrochemical properties of two α,α-sexithiophene compounds **1** and **2** (Figure 1). These molecules incorporate two photoresponsive units in the form of photoswitchable dithienylhexafluorocyclopentenes. These molecular photochromic switching units have proven their versatility in optoelectronic memory and display devices due to their fatigue resistance and thermal stability.[32–35] Surprisingly, despite the fact that the

* Corresponding author. E-mail: w.r.browne@rug.nl.
† FOM Institute for Atomic and Molecular Physics.
‡ University of Twente.

10.1021/jp8113896 CCC: $40.75
Published on Web 06/09/2009

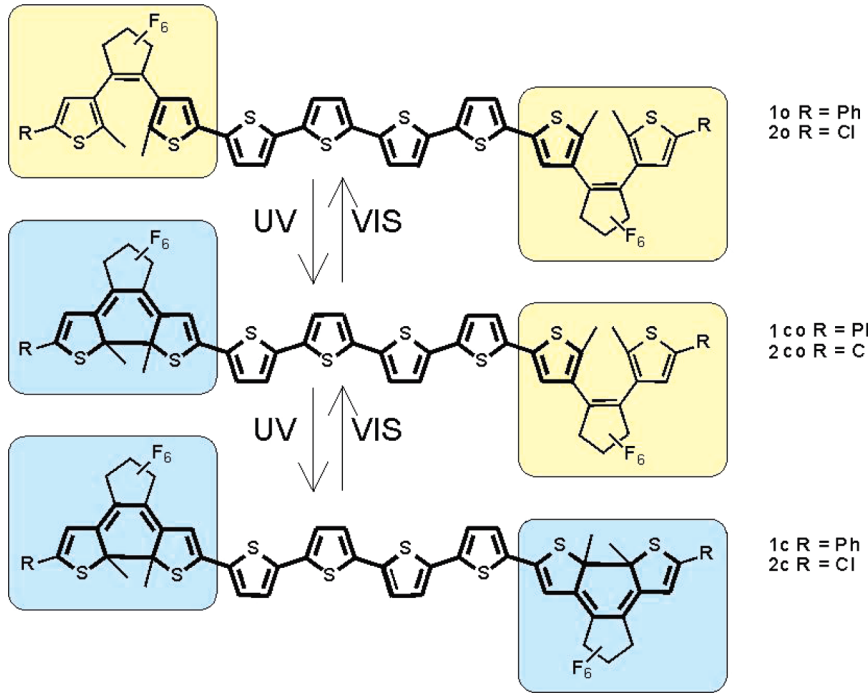

Figure 1. Molecular structures of compounds **1** and **2** in the fully open (**1o/2o**), singly closed (**1co/2co**), and fully closed (**1c/2c**) forms. Compound **1** is end-capped with peripheral phenyl groups and compound **2** with peripheral chloro groups. The suffixes o and c indicate that both photochromic units are in the open and closed states, respectively. The suffix oc indicates that one each of the photochromic units are in the open and closed state.

substituent (phenyl in **1** and Cl in **2**; Figure 1) on the outermost thiophene unit is well removed from the sexithiophene core, these substituents have a pronounced effect on the spectroscopic and electrochemical properties of the compounds, in particular on the energy of the HOMO level. However, to apply the functional behavior of these photochromic oligothiophenes, in particular in materials applications such as polymer modified electrodes,[36] it is essential that the effect of aggregation on their photochemical and photophysical properties be understood.

In the present study we investigate compounds **1** and **2** in their fully open states (Figure 1) by temperature dependent steady state and ultrafast time-resolved spectroscopies. Particular attention is paid to the effect of the peripheral substituents on aggregation phenomena. The steady state and transient spectroscopic techniques provide complementary information regarding the behavior of the compounds over the temperature range 120−298 K. As for the electrochemistry and steady state spectroscopy at room temperature, a considerable difference between the temperature dependent behaviors of **1** and **2** in the open form is noted. The results indicate that the hexafluorocyclopentene unit provides for effective electronic communication between the sexithiophene and the phenyl/chlorothienyl groups, and furthermore, provides for additional intermolecular interactions that can control aggregation properties in solution.

Experimental Section

n-Hexane, cyclohexane, isopentane (mp 113 K), and ethanol/methanol (4:1, T_g 115−125 K) were of spectroscopic grade or better and used as received. Hexane was used in room temperature steady state absorption spectra, cyclohexane was employed in the room temperature time-resolved measurements, and isopentane and ethanol/methanol were used in temperature dependent measurements. The synthesis and characterization of compounds **1o** and **2o** are reported elsewhere.[31] UV/vis spectra were recorded using a HP8453 diode array spectrophotometer or a JASCO V570 UV/vis-NIR spectrophotometer equipped with an integrating sphere for solid state measurements (JASCO-ISN470). Thin films, for solid state absorption spectra, were obtained by drop casting a dichloromethane solution of the compounds onto a glass slide. Fluorescence spectra were recorded on a JobinYvon Fluorolog MAX or a JASCO 7200 fluorometer. An Oxford Instruments OptistatDN was used for temperature dependent measurements. For the decomposition of the spectra into Gaussian bands, the nanometer scale was changed to reciprocal centimeters and the intensities of the spectra were corrected according to $I(\nu) = I(\lambda) \times \lambda^2$.[37] Fluorescence lifetime measurements were obtained using an Edinburgh Instruments F900n single photon counting instrument as described elsewhere.[38]

Time-resolved transient absorption spectroscopy was performed using an amplified Ti:Sapphire system (Clark CPA-2001) producing pulses at a 1 kHz rate. Part of the output was directed into a noncollinear optical parametric amplifier (NOPA) to generate near transform-limited pulses centered at 475 nm with a bandwidth of ∼30 nm. For compound **2o** the output of the amplified Ti:sapphire was frequency doubled to 388 nm. These pump pulses were used to excite the sample. Broadband probe pulses (450−750 nm) were obtained from a white light continuum (WLC) by focusing part of the output of the CPA into a 2 mm sapphire crystal. After passing through the sample, the WLC probe was directed into a spectrum analyzer (∼1 nm resolution) working at a 1 kHz detection rate and locked to the laser system. This fast detection system allowed for monitoring of the transient absorption signal on a shot-to-shot basis. Every other pump pulse was blocked by a chopper, providing a pump repetition rate of 500 Hz. At a given delay time between pump and probe pulses the pump induced changes in the absorption of the probe are detected as $\Delta OD = -\log(I_{\text{pump on}}/I_{\text{pump off}})$. The time resolution in the transient absorption measurements was

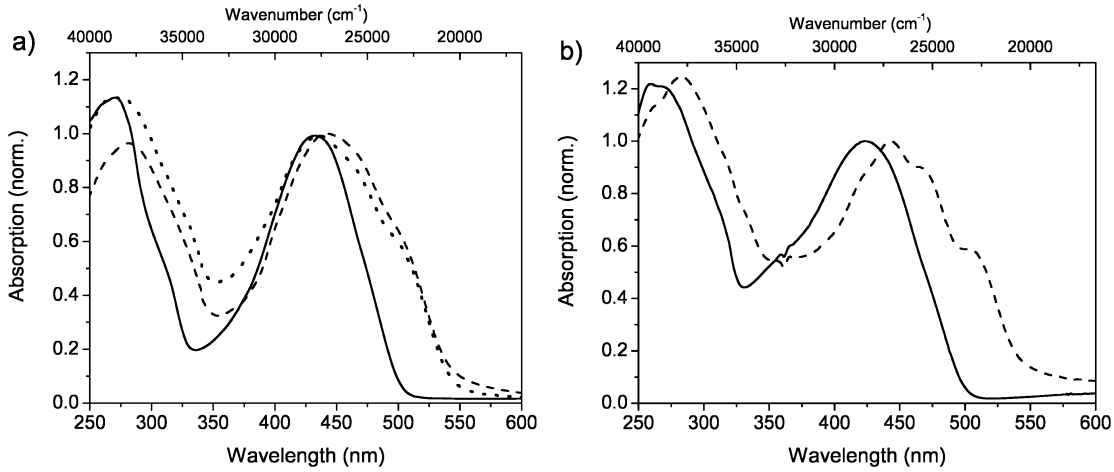

Figure 2. (a) Room temperature absorption spectra of **1o** in hexane (solid line), as a powder (dotted line), and as a drop cast film (dashed line). (b) Temperature dependent absorption spectra of **1o** in isopentane at 280 K (solid line) and 120 K (dashed line). Spectra in both panels are normalized with respect to the absorption band at ~430−450 nm.

determined by cross correlation to be 45 fs for excitation at 475 nm and ~100 fs at 388 nm. Room temperature measurements were collected using a 2 mm flow cell with a 50 mL reservoir to avoid the buildup of the photoproducts. Linear spectra of the samples before and after the time-resolved measurement were taken to ensure the absence of ring-closed species (Figure 1). Low temperature measurements were performed by placing the sample in a 1 mm cuvette and inserting it into a cryostat (Optistat CF, Oxford instruments), where it was cooled to 150 and 125 K for measurements in ethanol/methanol and isopentane, respectively. The excitation energy was limited to a maximum of 100 nJ for most measurements. The system response was linear (15−20% of the molecules are excited at an excitation power of 200 nJ) up to an excitation power of 100 μW (200 nJ per pulse). Kinetics obtained at 30 and 100 μW could be fitted with identical time constants.

Results and Discussion

Steady State Absorption Spectroscopy. The steady state absorption spectrum of **1o** in solution[31] and in the solid state as a powder and as a drop cast film at room temperature are shown in Figure 2a. In solution, the absorption spectrum consists of two absorption bands showing little structure. The solid state diffuse reflectance spectrum of a powdered solid sample is red-shifted and significantly more structured than the absorption spectrum in solution, suggesting partial ordering in the solid state. The absorption spectrum of a thin film of **1o** is comparable to that of the diffuse reflectance spectrum of the powdered solid. The spectral features in the solid state can be assigned to a vibronic progression as observed in other sexithiophene based systems at room and low temperature.[34] However, it is probable that in the solid state, either as a powder or a drop cast film, there will be a mixture of amorphous and microcrystalline material, the former reducing the resolution of the vibronic progression.

The temperature dependence of the absorption spectrum of **1o** in isopentane is shown in Figure 2b. The shape of the absorption spectrum is strongly temperature dependent; the absorption band undergoes a bathochromic shift of ~20 nm and shows resolved spectral features below 220 K. At 120 K, the main absorption band in the visible region, λ_{max} at ~430−440 nm, shows significant structure. The structure is similar, although considerably more pronounced compared to that observed in the (solid state) absorption and diffuse reflectance spectra.

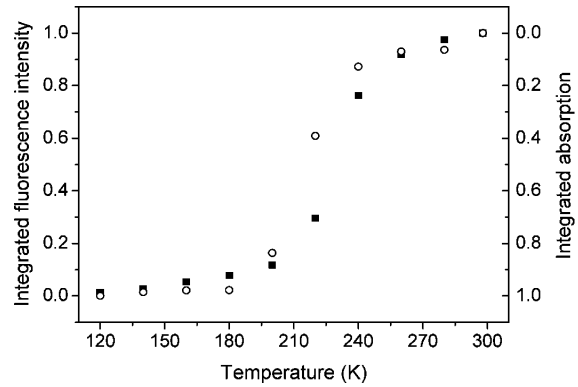

Figure 3. Temperature dependence of the absorption (circles) and fluorescence (squares) spectra of **1o** in isopentane. The fluorescence spectra are integrated over the range 450−800 nm and subsequently the intensity at a given temperature is scaled relative to that at 298 K. Similarly, the absorption spectra were integrated over the interval 443−550 nm. A constant background was subtracted, and the integrated spectra were scaled to that at 120 K.

Furthermore, the better resolution of the vibrational progression, in the absorption spectra of a solution at 120 K, compared with the solid state spectra suggest that the sample is aggregated with a greater degree of intermolecular order. The change in the visible spectrum from a broad unstructured absorption to a red-shifted structured spectrum occurs over a relatively narrow temperature range (180−220 K), well above the onset of the glass transition temperature of the solvent (~115 K) and is independent of concentration between 10^{-6} and 10^{-4} M (Figure 3 and Figure S2, Supporting Information).

Compound **1o** is strongly emissive in solution at room temperature ($\Phi_{fl} = 0.2$) and the fluorescence spectrum shows a vibrational progression typical of sexithiophenes (Figure 4).[39] The asymmetry between the featureless absorption and structured fluorescence spectra for oligothiophenes in solution has been noted previously.[40] The fluorescence spectrum is decomposed into three bands centered at 17 570, 18 690, and 19 980 cm^{-1}, corresponding to a vibrational progression of ~1100−1200 cm^{-1}. Comparison with the Raman and IR spectra of **1o**[31] indicates that the progression is coupled primarily to a C−C stretching vibration of the thiophene and that the emission originates from the sexithiophene unit. The Stokes shift in hexane is determined, by comparison of the origins of the deconvoluted absorption and fluorescence spectra (21 570 and

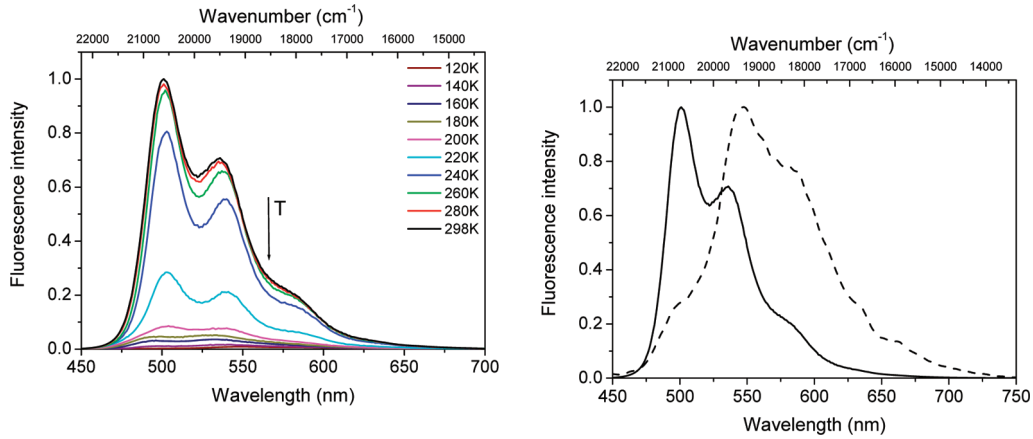

Figure 4. (a) Temperature dependence of the fluorescence of **1o** in isopentane. The excitation wavelength is 445 nm. (b) Fluorescence spectra at 300 K (solid) and 120 K (dash) normalized at the respective λ_{max}.

19 980 cm^{-1}, respectively), to be 1600 cm^{-1}. This value is less than the typical Stokes shift observed for unsubstituted oligothiophenes of 3000−3500 cm^{-1}.[41] In the solid state, either as a powder or a drop cast film, **1o** is essentially nonfluorescent (i.e., the intensity is of the same order of magnitude as the Raman scattering from the sample), in stark contrast to **1o** in solution.

The lack of fluorescence at low temperature and the increase in the resolution of the vibrational progression in the absorption spectra indicate that the molecules are assembled in an ordered structure. The X-ray single crystal diffraction structure of crystals of **1o** (grown from dichloromethane solution) was reported earlier.[31] The molecules are stacked with their long axis parallel making an angle to the horizontal (so-called herringbone structure). Molecules of **1o** stack together with an offset of one thiophene ring between the layers; i.e., the first thiophene of layer A lies below the second thiophene of layer B. This specific stacking of chromophores with their transition moments lying along their long axes, parallel to one another, is described as an H-aggregate.[42] In this type of aggregate the transition from the lowest exciton state to the ground state is optically forbidden due to symmetry selection rules.[15] Relaxation therefore occurs mainly via nonradiative processes resulting in a lower fluorescence quantum yield than observed in solution. Intermolecular interactions between the closely spaced molecules in these aggregates will cause splitting of the molecular energy levels into a series of exciton states.

Between 250 and 300 K, the fluorescence of **1o** is essentially temperature independent, but the fluorescence spectrum changes considerably between 200 and 250 K. Below 180 K the fluorescence is weak (∼1% of the intensity observed at 298 K) and has a distinctly different band shape (Figures 3 and 4). As with the temperature dependence of the absorption spectrum, this effect is still observed after a 30-fold decrease in concentration. The fluorescence spectrum obtained at 120 K is a sum of that of the weakly fluorescent aggregates of **1o** and of nonaggregated molecules of **1o**. After scaling and subtraction of residual fluorescence of nonaggregated **1o** (scaling at λ_{max} 501 nm, Figure 4b), the low temperature fluorescence spectrum was fitted with three Gaussian bands (16 350, 17 030, and 18 260 cm^{-1}). The apparent Stokes shift (i.e., the energy difference between the lowest absorption maximum and the maximum of the fluorescence spectrum) at 120 K is ∼2800 cm^{-1}. The sharp decrease in fluorescence indicates that aggregates are forming in solution upon decreasing temperature. Since this structural transition is characterized by the decrease in fluorescence, it is probable that H-aggregates, analogous to those observed previously in the X-ray crystal structure,[31] form in low temperature solutions. The effective absence of the 0−0 transition at 120 K (∼500 nm at room temperature, Figure 4b), which is forbidden in H-aggregates, provides additional support to this hypothesis.[43] However, formation of H-aggregates typically results in a blue shift in the absorption spectrum. In the present system the blue shift may be masked by conformational changes; i.e., the transition to the solid state is accompanied by increased planarity, resulting in the reduction in the contribution of torsional vibrational modes.[44]

Comparison between the Steady State Spectroscopy of 1o and 2o. As for **1o**, the lowest energy absorption band of **2o** at room temperature is decomposed into three bands, centered at 24 670, 27 640, and 30 780 cm^{-1}. However, the most noticeable difference in the effects of the peripheral chloro and phenyl groups is already visible in the absorption and fluorescence spectra at room temperature; for **2o**, the spectra are blue-shifted compared to **1o** (see Figure 5 for comparison, and Supporting Information for a complete set of spectra of **2o**). This implies that although the end groups are connected to the sexithiophene unit via an electron deficient alkene bond (by virtue of the electron withdrawing properties of the perfluorocyclopentene), electronic communication is not precluded. The temperature dependence of the integrated absorption spectrum of **2o** shows a gradual red shift and increase in intensity with decreasing temperature and the distinct phase transition observed for **1o** is absent.

The fluorescence of **2o** is less structured than that of **1o**. Nevertheless, the fluorescence spectrum can be decomposed into three bands centered at 18 800, 19 040, and 20 415 cm^{-1}, respectively. Again an abrupt temperature dependent phase transition in the fluorescence spectra is absent.

It is apparent that the phenyl substituent plays a key role in driving specific intermolecular interactions. Comparison with **2o** shows that aggregation occurs to a lesser extent, i.e., the intermolecular interactions are less strong, or that aggregates, different from those of **1o**, are formed. Hence minor changes to the peripheral groups affect aggregation behavior and consequently the temperature dependence of the luminescence properties can be tuned.

Transient Absorption Spectroscopy. Steady state spectroscopy indicated formation of H-aggregates at lower temperatures for **1o**, and to a lesser extent for **2o**. These results would predict a difference in the photoexcited state dynamics at low (125 K) and high (298 K) temperatures. To further elucidate the nature of these systems, their ultrafast dynamics were measured under

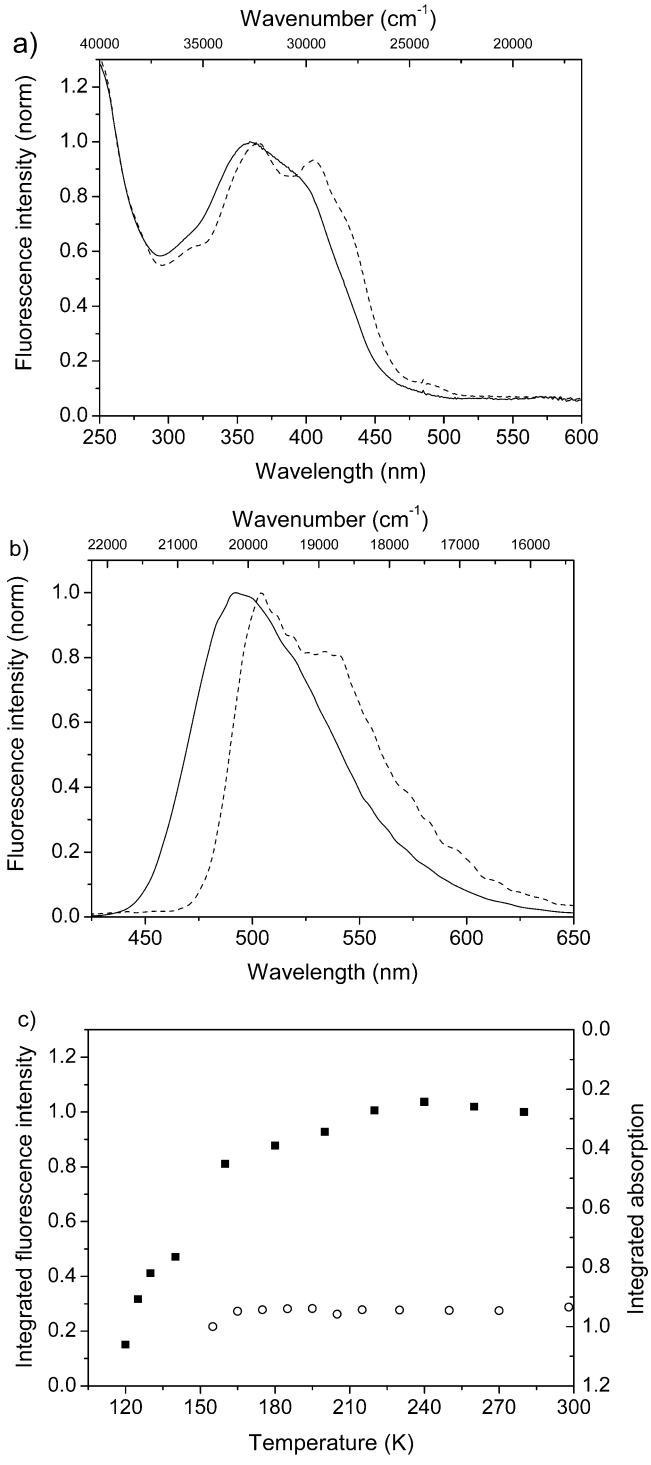

Figure 5. (a) Absorption spectra of **2o** in ethanol/methanol (1:4) at 280 K (solid line) and 120 K (dashed line). (b) Fluorescence spectra of **2o** at 280 K (solid line) and 120 K (dashed line). In panels a and b the spectra are normalized individually at their λ_{max} in the region ~350−370 and ~490−510 nm, respectively. (c) Integrated temperature dependent absorption spectra of **2o** in ethanol (circles) and integrated temperature dependent fluorescence spectra of **2o** in isopentane (squares).

a range of conditions. Transient absorption spectroscopy can provide deeper insight into the effect of the peripheral phenyl and chloro groups on aggregate formation. The steady state spectra assist in the assignment of features in the transient absorption spectra.[45]

Figure 6 shows the transient absorption spectra and single wavelength kinetic traces of **1o**. From the steady state absorption spectrum at 298 K (Figure 2) it is apparent that **1o** does not show significant absorption at wavelengths >500 nm; hence within the spectral window examined here (480−760 nm) ground state bleaching will not be observed. A structured negative signal (pump-induced transmission increase) is observed between 480 and 650 nm, while between 650 and 760 nm a positive signal (pump-induced absorption) dominates the spectrum. At longer time delays (>1 ns) the main spectral feature is a relatively narrow positive band centered at 700 nm. The negative signal in the transient spectra is comparable with the inverse of the steady state fluorescence spectrum of **1o** at room temperature (Figure 4 and gray shading Figure 6a), indicating that the negative transient signal is due to stimulated emission (SE) from the S_1 to S_0 state. The positive signal between 650 and 760 nm is assigned to excited state absorption (ESA) from S_1 to S_n, superimposed on a second signal at around at 700 nm, the nature of which cannot be assigned directly on the basis of the steady state spectra.

The decay over the whole spectral window can be fitted to a biexponential function with time constants of 35 ps (±6 ps) and 550 ps (±60 ps). The first time constant is tentatively assigned to a vibrational cooling process. The second time constant matches the fluorescence lifetime determined by single photon counting (600 ± 30 ps) and is similar to the lifetime of the lowest excited state in unsubstituted T6 in solution (800 ps)[46,47] and agrees closely with the lifetime of substituted T5 (300 ps).[46] Both SE and ESA regions can be fitted with identical decay constants, indicating that the ESA at ~750 nm is due to the S_1 to S_n transition. The signal at 700 nm grows in with a 550 ps time constant, hence the corresponding state must be populated from the S_1 state. The lifetime of the state centered at 700 nm is beyond the resolution of the present system (maximum scan range ~6 ns). However, the absence of a depletion at 700 nm prior to the t_0 of the pump−probe scan sets an upper limit for the lifetime of this state to be much less than the inverse of the repetition rate of the laser (500 μs). In assigning the transient absorption band at 700 nm, the formation of the monocationic state of the compound (**1o**$^+$ absorbs at ~750−800 nm)[48] or formation of **1c**, which absorbs at 640 nm, can be excluded. The rate of the process is typical of intersystem crossing (ISC) in oligothiophenes from a singlet to a triplet state.[49] The shape of the band compares closely with the T_1 to T_n transition in sexithiophene (T6)[48] in dichloromethane at 680 nm. Hence the positive signal in **1o** at 700 nm is assigned to the T_1 to T_n transition.

The transient spectra of **1o** recorded at 125 K are shown in Figure 7. The transient spectra are similar in certain respects to those observed at 298 K; i.e., negative signals are observed in the region 500−700 nm and a positive signal is seen at wavelengths longer than 700 nm. As at 298 K, the ESA at 700−750 nm is again assigned to the S_1−S_n transition. However, there are also distinct differences between the spectra at the two temperatures. The steady state absorption spectrum at 125 K is red-shifted compared to that at 298 K. The lowest energy absorption in the steady state absorption spectra of **1o** at 125 K is relatively intense at ~505 nm (Figure 2b) and falls within the spectral window examined (500−750 nm). Hence, in contrast to 298 K, a ground state bleaching signal is expected and indeed a negative signal centered at ~515 nm is observed in the transient spectra of **1o** at 125 K that is assigned to ground state bleaching of the S_0−S_1 transition.

The steady state fluorescence spectrum at 125 K is red-shifted compared with that observed at 298 K (Figure 4b). The transient spectra show a similar red shift in the SE signal with maxima

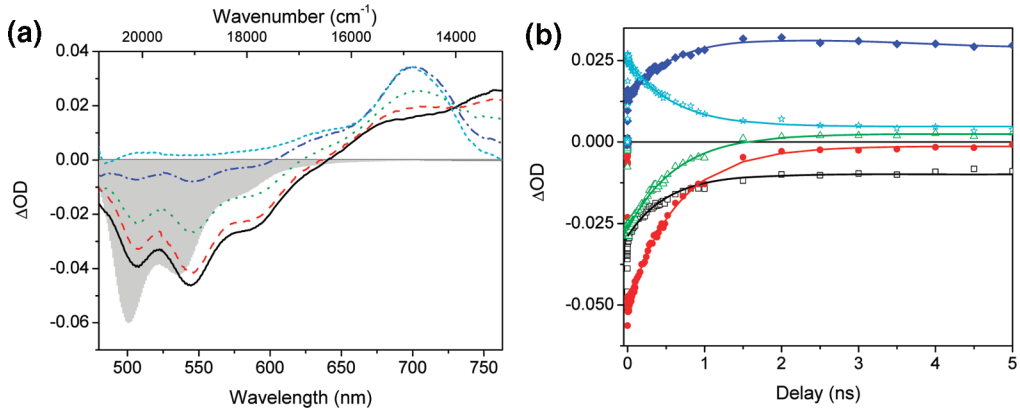

Figure 6. Transient absorption spectra of **1o** in cyclohexane $T = 298$ K. Pump 475 nm, 45 fs, 100 μW. (a) Spectral evolution of **1o** at 10 ps (solid line), 100 ps (dashed line), 320 ps (dotted line), 1 ns (dash-dotted line), and 4.5 ns (short dashed line). The inverted steady state fluorescence spectrum of **1o** is superimposed, with scaling (gray shading). (b) Temporal evolution of the transient signal at 450 (open squares), 545 (circles), 585 (open triangles), 685 (diamonds), and 750 (open stars) nm. The solid lines are the fits.

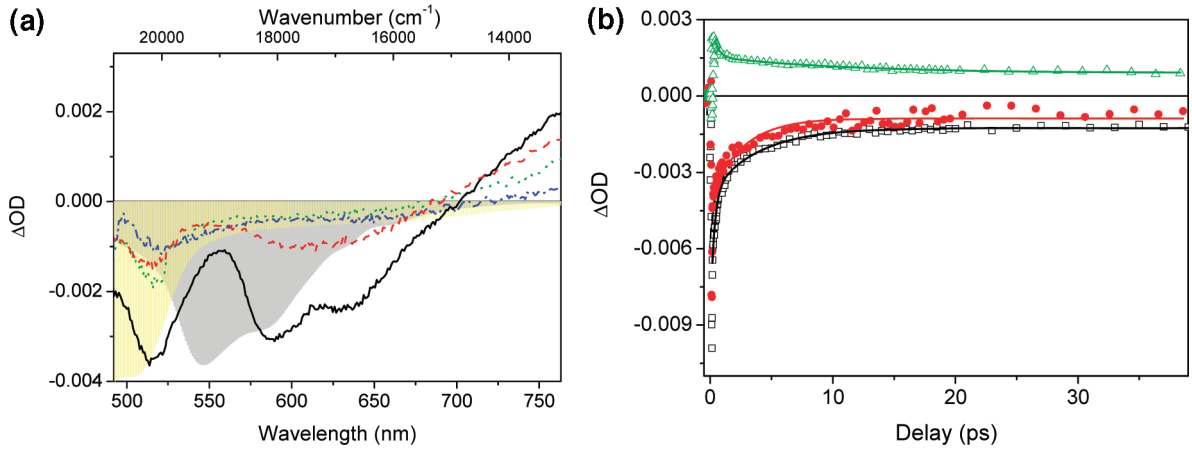

Figure 7. Transient absorption spectra of **1o** in isopentane $T = 125$ K. Pump 475 nm 45 fs, 30 nJ. (a) Spectral evolution of **1o** at 1 ps (solid line), 10 ps (dashed line), 100 ps (dotted line), and 4.5 ns (dash dotted line). The inverted steady state fluorescence and absorption spectra of **1o** at 125 K are superimposed, after scaling (dark and light gray shading respectively). (b) Temporal evolution of the transient signal at 515 (open squares), 615 (circles), and 750 (open triangles) nm. The solid lines are fitted to the data.

(i.e., at 1 ps after excitation in Figure 7a) at 544 and 588 nm at 298 and 125 K, respectively. Although the vibrational progression at 125 K differs between the transient SE and the steady state fluorescence spectra, the characteristic vibrational substructure remains recognizable (i.e., maxima at 588 and 631 nm for SE and 546, 588, 628, and 667 nm for the steady state fluorescence). The fact that not all the bands visible in the steady state fluorescence spectra are observed in the transient SE spectra can be explained by overlapping signals; i.e., ESA both at the red and the blue side of the SE can distort the shape compared with the steady state fluorescence spectrum.

The decrease in fluorescence intensity at low temperature (vide supra) was attributed to the formation of H-aggregates. Therefore, it is expected that the dynamics, observed at 125 and 298 K are different. The dynamics are considerably faster at 125 K with components of 650 fs ($\pm$170 fs) and 5.7 ps ($\pm$1.7 ps), Figure 7b. Additionally longer-lived signals are observed that have a smaller amplitude (by a factor of 4$-$40) than the fast components. These long-lived signals can be fitted with two components, i.e., 390 ps ($\pm$140 ps) and a time constant that is beyond the maximum scan range of the system, but with an upper limit of $\ll$500 μs. The sharp decrease in the transient signal that is observed especially at 515 nm (Figure 7b) is not assigned to ultrafast kinetics in the system but instead to a coherent artifact. The presence of two distinct species, one in the aggregated state and a small amount as isolated molecules, is based on the assignment of the several decay time constants at 125 K. The latter, as seen at 298 K, give rise to the $\sim$400 ps and $\ll$500 μs decay times. Therefore, the faster time constants are characteristic of the aggregated species with efficient nonradiative deactivation expected due to the intermolecular interactions present. The fastest time constant of 650 fs is assigned to rapid relaxation to the lowest vibrational state in S_1.[50–52] The nature of the state that decays with the 5.7 ps time constant is unclear. Lanzani et al. tentatively attributed a similar picosecond time constant to charge separation.[46] It is perhaps more probable that there are local defects and impurities in the H-aggregates that cause the trapping of the excited excitons after rapid intermolecular energy transfer. Figure 8 shows tentative energy diagrams for the molecules and the aggregates.

Comparison between the Transient Absorption Spectroscopy of 1o and 2o. Table 1 shows the results of the fitting of the transients in **1o** and **2o**. At room temperature the different bands in the transient spectra agree well with those observed for **1o**. As expected, the spectral features mirror the steady state spectra, and therefore, the SE in **2o** shows few spectral features (Figure S6, Supporting Information). The three time constants that are needed to fit the transients in **2o** are similar and have the same physical origin as those of **1o**. The excited state lifetime in **2o** is considerably longer than in **1o**. A possible explanation is a difference in the destabilization of the planar configuration of the molecules by the subsituent.[46] Along these lines, the

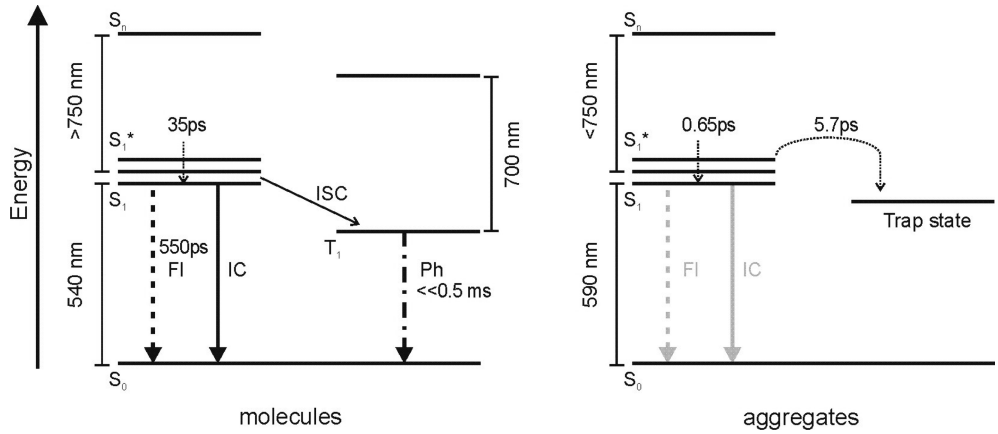

Figure 8. Energy diagram for **1o** in the form of isolated molecules (left) and aggregates (right). At room temperature only isolated molecules are present, while aggregation is observed at lower temperatures. At low temperatures there is a mixture of a (minor fraction of) isolated molecules and of the aggregates. Therefore, at 125 K both energy level diagrams are relevant and a combination of time constants, long for the isolated molecules and short for the aggregates, and spectral features belonging to both cases can be expected in the transient absorption experiments at low temperatures.

TABLE 1: Transient Absorption Kinetics from Exponential Fits for 1o and 2o

	T (K)	decay constant	($\pm$[a])		T (K)	decay constant	($\pm$[a])
1o	298	35 ps	6 ps	**2o**	298	8.3 ps	3.2 ps
		550 ps	60 ps			1.3 ns	0.4 ns
		$\ll$500 μs				$\ll$500 μs	
1o	125	650 fs	170 fs	**2o**	125	8.6 ps	1.7 ps
		5.7 ps	1.7 ps			1.5 ns	0.3 ns
		390 ps	140 ps				
		$\ll$500 μs					

[a] The uncertainties in the decay constants are determined by fitting ~20 transients per experiment. The standard deviation of these fits was taken as the uncertainty.

chloro substituent allows for more planar molecules, lowering the efficiency of low energy torsional modes as acceptor modes in the radiationless decay to the ground state. The shape of the triplet state in **2o**, unlike the distinct band around 700 nm in **1o**, is spread out over the whole spectrum.

The transients of **2o** at 125 K are of poorer quality, due to the low concentrations achievable in solution. However, it is clear that a short time constant dominates the dynamics. The presence of an 8 ps time constant in both the 298 and the 125 K transients appears to be coincident; however, the quality of the data precludes identification of a similar subpicosecond time constant as in **1o**.

The results from steady state spectroscopy could not discriminate between the formation of aggregates showing smaller intermolecular interactions or different types of aggregates in **1o** and **2o**. The decrease in fluorescence intensity in **2o** indicated the formation of H-aggregates. Moreover, no additional spectral features typical for different arrangements such as J-aggregates, superradiance, and a narrow J-aggregate peak, were observed.[17] However, the time-resolved data provide a definite answer. While for **1o** the temperature dependence of the transient absorption decay time constants is indicative of aggregation, the data are less clear for **2o**. The decay time constants at 298 and 125 K are coincidently similar; however, the amplitudes are not. As for **1o**, the amplitude of the fast component at 125 K in **2o** exceeds the amplitude of the long component. On the basis of this similarity, we conclude that H-aggregates are formed by both compounds. Nevertheless, the intermolecular interactions are stronger for **1o**, indicating that the phenyl group in **1o** contributes considerably to the intermolecular interactions by additional $\pi-\pi$ interactions.

Conclusion

We have studied two α-substituted sexithiophene compounds with two peripheral side groups (i.e., phenyl and chloro) in solution under several different conditions by steady state and time-resolved spectroscopies. The absorption, fluorescence, and transient spectra of **1o** and their respective temperature dependence manifest the formation of aggregates upon decreasing temperature. While at 298 K the system consists of isolated molecules, below 180 K specific intermolecular interactions drive the system to form H-aggregates. Likewise, H-aggregates have also been observed in solid state samples of **1o** as revealed by absorption and X-ray spectroscopy. Analogue measurements of **2o** indicate a markedly different aggregation behavior; quenching of the fluorescence was not complete and occurred gradually over the whole temperature range. The transient spectral data for **1o** and **2o** at 125 K provides strong evidence that both compounds form H-aggregates. Nevertheless, the interactions between the molecules of **2o** are weaker and lack the potential for $\pi-\pi$ stacking of the peripheral phenyl rings of **1o**. This result leads to the conclusion that there is a pronounced effect of the peripheral substituent (i.e., phenyl vs chloro) on both the electronic and aggregative properties of these systems. The hexafluorocyclopentene groups facilitate communication between the sexithiophene and the chloro and phenyl-substituted monothiophene unit. These results demonstrate that well-structured intermolecular aggregation can be achieved in the absence of more traditional functional units such as amides and ureas. Furthermore, these data provide an understanding of the electronic properties of these compounds essential to their application in multicomponent molecular systems.

Acknowledgment. This work is part of the research program of the Stichting Fundamenteel Onderzoek der Materie (Foundation for Fundamental Research on Matter) with financial support from NanoNed and the Nederlandse Organisatie voor Wetenschappelijk Onderzoek (Netherlands Organisation for Scientific Research). J.L.H. and W.R.B. acknowledge support from NWO through Vidi grants.

Supporting Information Available: Temperature dependent absorption and fluorescence spectra of **1o** and **2o**. This material is available free of charge via the Internet at http://pubs.acs.org.

References and Notes

(1) Chiang, C. K.; Fincher, C. R.; Parker, Y. W.; Heeger, A. J.; Shirakawa, H.; Louis, E. J.; Gau, S. C.; MacDiarmid, A. G. *Phys. Rev. Lett.* **1977**, *39*, 1098–1101.

(2) Garnier, F. *Acc. Chem. Res.* **1999**, *32*, 209–215.

(3) Garnier, F.; Hajlaoui, R.; Yassar, A.; Srivastava, P. *Science* **1994**, *265*, 1684–1686.

(4) Nishida, J.; Miyagawa, T.; Yamashita, Y. *Org. Lett.* **2004**, *6*, 2523–2526.

(5) Gazotti, W. A., Nogueira A. F., Girotto, E. M., Micaroni, L., Martini, M. das Neves, S., De Paoli, M. *Handbook of Advanced Electronic and Photonic Materials and Devices*; Academic Press: San Diego, CA, 2001.

(6) Durmus, A.; Gunbas, G. E.; Camurlu, P.; Toppare, L. *Chem. Commun.* **2007**, 3246–3248.

(7) Berridge, R.; Wright, S. P.; Skabara, P. J.; Dyer, A.; Steckler, T.; Argun, A. A.; Reynolds, J. R.; Ross, W. H.; Clegg, W. *J. Mater. Chem.* **2007**, *17*, 225–231.

(8) Roncali, J. *Chem. Rev.* **1992**, *92*, 711–738.

(9) Lorcy, D.; Cava, M. P. *Adv. Mater.* **1992**, *4*, 562–564.

(10) Klauk, H. *Organic Electronics*; Wiley-VCH: Weinheim, Germany, 2006.

(11) For a detailed study of the ultrafast spectroscopy of a-sexithiophene see: Watanabe, K.; Asahi, T.; Fukumura, H.; Masuhara, H.; Hamano, K.; Kurata, T. *J. Phys. Chem. B* **1997**, *101*, 1510–1519.

(12) Bauerle, P. *Electronic Materials: The Oligomer Approach*; Wiley-VCH: Weinheim, Germany, 1998.

(13) Roncali, J. *Acc. Chem. Res.* **2000**, *33*, 147–156.

(14) Tour, J. M. *Acc. Chem. Res.* **2000**, *33*, 791–804.

(15) Da Como, E.; Loi, M. A.; Murgia, M.; Zamboni, R.; Muccini, M. *J. Am. Chem. Soc.* **2006**, *128*, 4277–4281.

(16) Westenhoff, S.; Abrusci, A.; Feast, W. J.; Henze, O.; Kilbinger, A. F. M.; Schenning, A. P. H. J.; Silva, C. *Adv. Mater.* **2006**, *18*, 1281–1285.

(17) Clark, J.; Silva, C.; Friend, R. H.; Spano, F. C. *Phys. Rev. Lett.* **2007**, *98*, 206406.

(18) Feng, Y. F.; Yan, Y. L.; Wang, S.; Zhu, W. H.; Qian, S. X.; Tian, H. *J. Mater. Chem.* **2006**, *16*, 3685–3692.

(19) Alberti, A.; Ballarin, B.; Guerra, M.; Macciantelli, D.; Mucci, A.; Parenti, F.; Schenetti, L.; Seeber, R.; Zanardi, C. *ChemPhysChem* **2003**, *4*, 1216–1225.

(20) Bauerle, P.; Segelbacher, U.; Maier, A.; Mehring, M. *J. Am. Chem. Soc.* **1993**, *115*, 10217–10223.

(21) Fichou, D. *Handbook of Oligo- and Polythiophenes*; Wiley-VCH: New York, 1999.

(22) Katz, H. E.; Bao, Z. N.; Gilat, S. L. *Acc. Chem. Res.* **2001**, *34*, 359–369.

(23) Sonmez, G.; Sonmez, H. B.; Shen, C. K. F.; Jost, R. W.; Rubin, Y.; Wudl, F. *Macromolecules* **2005**, *38*, 669–675.

(24) Schwendeman, I.; Hickman, R.; Sonmez, G.; Schottland, P.; Zong, K.; Welsh, D. M.; Reynolds, J. R. *Chem. Mater.* **2002**, *14*, 3118–3122.

(25) van Hutten, P. F.; Wildeman, J.; Meetsma, A.; Hadziioannou, G. *J. Am. Chem. Soc.* **1999**, *121*, 5910–5918.

(26) Schenning, A. P. H. J.; Kilbinger, A. F. M.; Biscarini, F.; Cavallini, M.; Cooper, H. J.; Derrick, P. J.; Feast, W. J.; Lazzaroni, R.; Leclère, P.; McDonnell, L. A.; Meijer, E. W.; Meskers, S. C. J. *J. Am. Chem. Soc.* **2002**, *124*, 1269–1275.

(27) Tsivgoulis, G. M.; Lehn, J. M. *Chem.—Eur. J.* **1996**, *2*, 1399–1406.

(28) Tsivgoulis, G. M.; Lehn, J. M. *Adv. Mater.* **1997**, *9*, 39–42.

(29) Peters, A.; McDonald, R.; Branda, N. R. *Chem. Commun.* **2002**, *19*, 2274–2275.

(30) (a) Tanifuji, N.; Irie, M.; Matsuda, K. *Chem. Lett.* **2005**, *34*, 1580–1581. (b) Zhao, W.; Carreira, E. M. *Chem.—Eur. J.* **2007**, *13*, 2671–2685. (c) Xie, N.; Chen, Y. *New J. Chem.* **2006**, *30*, 1595–1598. (d) Ortica, F.; Smimmo, P.; Favaro, G.; Mazzucato, U.; Delbaere, S.; Venec, D.; Vermeersch, G.; Frigoli, M.; Moustrou, C.; Samat, A. *Photochem. Photobiol. Sci.* **2004**, *3*, 878–885. (e) Frigoli, M.; Pimienta, V.; Moustrou, C.; Samat, A.; Guglielmetti, R.; Aubard, J.; Maurel, F.; Micheau, J.-C. *Photochem. Photobiol. Sci.* **2003**, *2*, 888–892. (f) Yassar, A.; Jaafari, H.; Rebiere-Galy, N.; Frigoli, M.; Moustrou, C.; Samat, A.; Guglielmetti, R. *Eur. Phys. J: Appl. Phys.* **2002**, *18*, 3–8. (g) Yassar, A.; Rebiere-Galy, N.; Frigoli, M.; Moustrou, C.; Samat, A.; Guglielmetti, R.; Jaafari, A. *Synth. Met.* **2001**, *124*, 23–27. (h) Matsuda, K.; Matsuo, M.; Irie, M. *J. Org. Chem.* **2001**, *66*, 8799–8803. (i) Irie, M.; Uchida, K. *Bull. Chem. Soc. Jpn.* **1998**, *71*, 985–996.

(31) Areephong, J.; Hurenkamp, J. H.; Milder, M. T. W.; Meetsma, A.; Herek, J. L.; Browne, W. R.; Feringa, B. L. *Org. Lett.* **2009**, *11*, 721–724.

(32) Feringa, B. L. *Molecular Switches*; Wiley-VCH: Weinheim, 2001.

(33) Yao, J. N.; Hashimoto, K.; Fujishima, A. *Nature* **1992**, *355*, 624–626.

(34) Tian, H.; Yang, S. J. *Chem. Soc. Rev.* **2004**, *33*, 85–97.

(35) Irie, M. *Chem. Rev.* **2000**, *100*, 1685–1716.

(36) Areephong, J.; Kudernac, T.; de Jong, J. J. D.; Carroll, G. T.; Pantorotta, D.; Hjelm, J.; Browne, W. R.; Feringa, B. L. *J. Am. Chem. Soc.* **2008**, *130*, 12850–12851.

(37) Lakowicz, J. R. *Principles of Fluoresence spectroscopy*, 2nd ed.; Kluwer Academic/Plenum Publishers: New York, 1999.

(38) Browne, W. R.; O'Boyle, N. M.; Henry, W.; Guckian, A. L.; Horn, S.; Fett, T.; O'Connor, C. M.; Duati, M.; De Cola, L.; Coates, C. G.; Ronayne, K. L.; McGarvey, J. J.; Vos, J. G. *J. Am. Chem. Soc.* **2005**, *127*, 1229–1241.

(39) Yassar, A.; Horowitz, G.; Valat, P.; Wintgens, V.; Hmyene, M.; Deloffre, F.; Srivastava, P.; Lang, P.; Garnier, F. *J. Phys. Chem.* **1995**, *99*, 9155–9159.

(40) The broadness and generally blue-shifted absorption spectrum of oligothiophenes observed in solution, compared with their solid state absorption spectra, has been assigned as due to the involvement of low energy out of plane torsional modes which are essentially "locked out" in the solid state. For a detailed discussion see: (a) Gierschner, J.; Mack, H. G.; Luer, L.; Oelkrug, D. *J. Chem. Phys.* **2002**, *116*, 8596–8609. (b) Gierschner, J.; Mack, H. G.; Egelhaaf, S. S.; Doser, B.; Oelkrug, D. *Synth. Met.* **2003**, *138*, 311–315. (c) Ellinger, S.; Kreyes, A.; Ziener, U.; Hoffmann-Richter, C.; Landfester, K.; Möller, M. *Eur. J. Org. Chem.* **2007**, 5686–5702.

(41) Chosrovian, H.; Rentsch, S.; Grebner, D.; Dahm, D. U.; Birckner, E.; Naarmann, H. *Synth. Met.* **1993**, *60*, 23–26.

(42) May, V., Kühn, O. *Charge and Energy Transfer Dynamics in Molecular Systems*; Wiley-VCH: Berlin, Germany, 2000.

(43) Oelkrug, D.; Egelhaaf, H. J.; Gierschner, J.; Tompert, A. *Synth. Met.* **1996**, *76*, 249–253.

(44) Cornil, J.; Beljonne, D.; Calbert, J. P.; Bredas, J. L. *Adv. Mater.* **2001**, *13*, 1053–1067.

(45) At low temperature, there is no evidence of ring closing, even after prolonged (>2 h) irradiation at 365 nm. Hence, at these temperatures ring closing reactions are not observed in the spectroscopic studies. Furthermore, time-resolved spectra show that even at room temperature the ring closing reaction and resulting permanent absorption changes are negligible.

(46) Lanzani, G.; Cerullo, G.; Stagira, S.; De Silvestri, S. *J. Photochem. Photobio. A: Chem.* **2001**, *144*, 13–19.

(47) Colditz, R.; Grebner, D.; Helbig, M.; Rentsch, S. *Chem. Phys.* **1995**, *201*, 309–320.

(48) Wintgens, V.; Valat, P.; Garnier, F. *J. Phys. Chem.* **1994**, *98*, 228–232.

(49) Becker, R. S.; deMelo, J. S.; Maçanita, A. L.; Elisei, F. *J. Phys. Chem.* **1996**, *100*, 18683–18695.

(50) Yang, J. P.; Paa, W.; Rentsch, S. *Chem. Phys. Lett.* **2000**, *320*, 665–672.

(51) Lap, D. V.; Grebner, D.; Rentsch, S. *J. Phys. Chem. A* **1997**, *101*, 107–112.

(52) Lanzani, G.; Nisoli, M.; De Silvestri, S.; Tubino, R. *Chem. Phys. Lett.* **1996**, *251*, 339–345.

JP8113896